

Effects of solar radiation on dimethylsulfide cycling in the western Atlantic Ocean

D.A. Toole^{a,*}, D. Slezak^{b,c}, R.P. Kiene^{b,c}, D.J. Kieber^d, D.A. Siegel^a

^a*Institute for Computational Earth System Science, University of California, Santa Barbara, CA 93106, USA*

^b*Department of Marine Sciences, University of South Alabama, Mobile, AL 36688, USA*

^c*Dauphin Island Sea Lab, Dauphin Island, AL 36528, USA*

^d*Chemistry Department, College of Environmental Science and Forestry, State University of New York, Syracuse, NY 13210, USA*

Received 19 November 2004; received in revised form 29 July 2005; accepted 2 September 2005

Available online 9 November 2005

Abstract

The influence of solar radiation on springtime rates of photochemical and biological consumption of dimethylsulfide (DMS) in surface waters from the western Atlantic Ocean was examined by exposing 0.2 μm filtered and unfiltered surface seawater to natural sunlight at five depths in the upper 30 m. Parallel deck incubations of 0.2 μm filtered seawater under various long-pass optical filters were also carried out to aid in assessing the wavelength dependence of DMS photolysis. DMS photolysis rate constants for mid-day exposure ($\sim 10:30$ – $17:30$ local time) to surface irradiance ranged from 0.026 to 0.086 h^{-1} and were highest in coastal and shelf waters. Photolysis rate constants decreased with increasing irradiation depth, in accordance with the attenuation of ultraviolet radiation (UVR, 280–400 nm). Total DMS consumption rates (photochemical + biological) in unfiltered surface samples also decreased with increasing incubation depth and were larger than photolysis rates at nearly all depths and all stations. The decrease in photolysis rate constants with exposure depth was mirrored by biological DMS consumption rate constants that were severely inhibited at surface irradiances, and approached or exceeded dark rate constants at deeper exposure depths. Photolysis rates were 2–19 times greater than estimated biological consumption rates in the surface light exposed samples, while biological consumption rates were significantly larger than photolysis rates at incubation depths below the 1% light level for UV–B radiation (280–320 nm). Total DMS loss rates increased up to nine-fold with UVR exposure, but changes in DMS concentrations were not strongly correlated to light dose, presumably due to parallel, light-mediated DMS production processes. The primary loss process for DMS depended mainly on the depth interval considered and the attenuation of UVR; in general, photochemical removal dominated shallow layers characterized by high UV–B intensities, whereas biological removal dominated in deeper layers where UV–B was absent, but UV–A (320–400 nm) and visible (400–700 nm) light fluxes were still relatively high. These results demonstrate that UVR exposure significantly influences the spatial and temporal pattern of DMS production and loss processes, and ultimately the DMS flux to the atmosphere.

© 2005 Elsevier Ltd. All rights reserved.

Keywords: Sulfur compounds; Dimethylsulfide; Ultraviolet radiation; Photochemistry; Rate constants; Light attenuation; North Atlantic; Sargasso Sea; Gulf of Maine

*Corresponding author. Present address: Department of Marine Chemistry and Geochemistry, Woods Hole Oceanographic Institution, Woods Hole, MA 02543, USA. Tel.: +1 508 289 3552; fax: +1 508 457 2193.

E-mail address: dtoole@whoi.edu (D.A. Toole).

1. Introduction

The biogeochemical cycling of reduced sulfur compounds between the upper water column and the marine atmosphere has been implicated in a cloud-albedo feedback loop (e.g. Charlson et al., 1987; Shaw, 1983). This hypothesized climate regulation mechanism suggests that as upper-ocean temperatures and radiation exposure increase, marine communities may respond by increasing production of the volatile organic sulfur compound dimethylsulfide (DMS) and its precursor dimethylsulfoniopropionate (DMSP). The atmospheric oxidation products of DMS are sulfate aerosols which can function as new cloud condensation nuclei or promote the growth of existing condensation particles thereby directly, and indirectly, reducing the solar radiation reaching the ocean surface (Ayers and Gillett, 2000; Charlson et al., 2000). The sea-air ventilation of biologically produced DMS also contributes to the background levels of tropospheric sulfate aerosols in the remote marine atmosphere (Andreae and Crutzen, 1997), and is potentially involved in the autocatalytic activation of ozone-destroying halogens (Ayers and Gillett, 2000), reinforcing potential radiative and climatic impacts. As a result, alterations in the oceanic biogeochemical cycling of DMS, and the resulting flux to the atmosphere, could alter the radiative properties of the atmosphere. Understanding how the biogeochemical cycling of reduced sulfur compounds, and ultimately their emission to the atmosphere, varies in response to physical forcing such as light and mixing is critical to assessing the feedback mechanisms put forth in the climate regulation hypothesis.

DMS concentrations are the product of a complex and dynamic network of production and loss processes that span the entire foodweb and occur on a variety of scales including physical and chemical cycling mechanisms (e.g. Simó, 2004). Very few studies have investigated the mechanisms involved in how light affects DMS cycling processes and concentrations. Most efforts have focused on phytoplankton intracellular DMS and DMSP production (e.g. Slezak and Herndl, 2003; Sunda et al., 2002; van Rijssel and Gieskes, 2002) or the impact of variations in mixed layer depth (e.g. Simó and Dachs, 2002; Simó and Pedrós-Alió, 1999a). Mixed layer DMS is removed via three primary mechanisms: photolysis (e.g. Brimblecombe and Shooter, 1986; Brugger et al., 1998; Kieber et al., 1996; Toole et al., 2003), biological consumption by microbes

(e.g. González et al., 2000; Kiene and Bates, 1990; Zubkov et al., 2002), and sea-air ventilation (e.g. Zemmelen et al., 2004). Photolysis is a direct function of irradiance dose and can make an important contribution to the temporal and spatial variability of upper-ocean DMS (e.g. Kieber et al., 1996; Toole et al., 2003, 2004). Although some studies have alluded to it (e.g. Sakka et al., 1997; Simó and Pedrós-Alió, 1999a), only Slezak et al. (2001) specifically studied the effects of light on biological DMS consumption rates. They compared biological and photochemical removal rates of DMS in seawater from the Adriatic and coastal North Sea and found that in samples exposed to surface levels of irradiation, biological DMS consumption rates were $\sim 40 \pm 14\%$ of the dark biological consumption rates. Additionally, while sea-air ventilation is not directly impacted by variations in the incident light flux, secondary effects via solar heating of the oceanic surface layer and changes in the depth of the mixed layer will impact rates. Supporting this, Simó and Pedrós-Alió (1999b) observed significant short-term variability in biological and sea-air loss rates of DMS, and estimated DMS photolysis rates, in response to short-term changes in solar radiation and wind speed.

All three primary DMS loss mechanisms are important under different environmental conditions, but our understanding of how they vary in response to physical forcing such as light and mixing is poor. To this end, we measured DMS photolysis and biological consumption rates utilizing a free-floating drifter array that exposed surface seawater samples to natural light at a variety of depths in the upper 30 m of the western Atlantic Ocean. We sampled a diverse range of water masses and included ancillary biophysical measurements such as incident flux and water column attenuation of solar ultraviolet radiation (UVR, 280–400 nm) and visible radiation (400–700 nm), wind speed, temperature, and light absorption by chromophoric dissolved organic matter (CDOM). The goals of our study were to quantify the role of light in mediating DMS loss processes and to develop biophysical parameterizations appropriate for inclusion in modeling studies.

2. Materials and methods

2.1. Shipboard sample collection

Seawater samples encompassing a range of environments and conditions were collected at 15

western Atlantic Ocean stations in April 2002 aboard the R/V *Oceanus* (Fig. 1; Table 1). Free-floating drifter deployments for in-water DMS photolysis and total consumption rate determinations were made at six stations (further detail provided below). At each station vertical profiles of samples from the upper 100 m were collected with 10 L Niskin bottles during early morning (~06:00) hydrocasts with a conductivity, temperature, and depth (CTD) rosette. Routine measurements at each station and depth included concentrations of chlorophyll *a*, dissolved inorganic nutrients, algal accessory pigments, DMS, particulate and dissolved dimethylsulfoniopropionate (pDMSP and dDMSP, respectively), and dawn to dusk monitoring of wavelength resolved incident irradiance ($E_d(0^+, \lambda)$, UV and visible channels). CDOM absorbance and dissolved organic carbon (DOC) concentration were sampled at the surface only. The shipboard underway system continuously monitored and recorded a variety of ancillary data including sea surface temperature (SST), salinity, wind speed, and wind direction. During drifter array deployments, vertical profiles of spectral downwelling irradiance and upwelling radiance ($E_d(z, \lambda)$ and $L_u(z, \lambda)$, respec-

tively) were sampled periodically throughout the day.

All seawater samples were drawn from the Niskin bottles using Masterflex silicone tubing that had been rinsed with reagent grade 10% hydrochloric acid (HCl), copiously rinsed in Milli-Q water, and thoroughly dried. All Teflon, polycarbonate, and glass sample collection bottles were rinsed with 10% HCl, rinsed three times with Milli-Q water, and rinsed five times with seawater before sample collection. Amber glass vials for CDOM analysis were cleaned with three rinses of Milli-Q water followed by three rinses each of 10% hydrofluoric acid, 10% HCl, and 10% methanol (all reagent grade or better). The CDOM glassware was copiously rinsed with Milli-Q water to remove any chemical residue and baked in a muffle furnace at 550 °C for at least 6 h. Filtered water for DMS photolysis incubations and CDOM absorbance determinations was obtained directly from the Niskin bottles by in-line filtration through 142 mm, 0.22 μm Millipore polycarbonate membrane filters using a polycarbonate filter apparatus (Geotech). Before sample collection, all filters were flushed with at least 1 L Milli-Q water and 0.5 L seawater sample to eliminate any organic material potentially leaching from the filter (Carlson and Ducklow, 1996). For CDOM analysis, the filtered seawater samples were stored in the dark at 4 °C for the duration of the cruise pending transfer to the laboratory in Syracuse, New York. CDOM absorbances were determined using a Hewlett-Packard 8453 UV–VIS photodiode array spectrophotometer equipped with a 5 cm quartz microliter flow cell (Hellma), with Milli-Q water as the reference (wavelength range scanned = 200–1100 nm). Absorbance curves were corrected for offsets (assumed zero between 675 and 700 nm) and fit using a standard CDOM exponential functional relationship; CDOM absorption coefficients ($a_{\text{CDOM}}(\lambda)$) were calculated according to Green and Blough (1994). DOC samples were also filtered directly from the CTD Niskin bottles, through precombusted GF/F filters, using silicone tubing and metal free polycarbonate Swinex filter housings which had been cleaned with 10% HCl and copious rinses with Milli-Q water. The filtrate was frozen in an organics-free freezer and at the end of the cruise shipped to the University of California, Santa Barbara DOC analysis laboratory. All DOC samples were analyzed on a modified Shimadzu TOC V (Carlson et al., 2002).

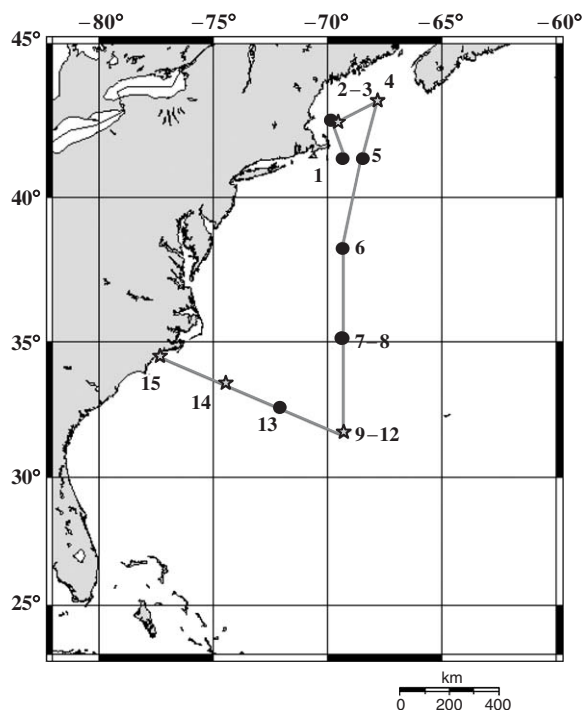


Fig. 1. Hydrographic stations in the western Atlantic Ocean. Free-floating drifter array incubation data are available from stations 3, 4, 11, 12, 14, and 15 (denoted by gray stars).

Table 1
Incubation details

Day in April 2002	Station	Drifter array incubation time	Deck-box incubation time	Clouds	DMS	pDMSP	dDMSP	NO ₃ ⁻	Chl <i>a</i>	MLD
7	3	12:00–17:11	12:34–16:40	Clear	0.63	9.9	2.7	7.89	0.93	42
8	4	10:45–17:10	10:39–17:15	Overcast	0.70	18.7	4.3	5.42	0.99	47
10	6	—	10:55–16:33	Dark high clouds	6.40	33.3	4.3	0.62	1.14	20
11	7	—	10:39–16:59	High thin clouds	1.34	14.1	3.0	0.12	0.31	47
12	8	—	10:07–15:38	Dark high clouds	2.28	24.1	2.4	0.09	0.22	6
15	11	10:41–17:08	09:49–17:00	Clear	2.10	6.7	2.4	0.15	0.05	21
16	12	10:43–17:58	09:54–16:21	Clear	3.35	6.2	1.8	0.22	0.04	11
17	13	—	10:10–17:32	Clear	2.79	10.4	3.6	0.17	0.10	9
18	14	09:57–18:08	09:20–16:57	Clear	2.43	14.6	4.2	0.10	0.06	7
19	15	10:52–17:19	10:10–16:52	Clear	1.43	8.1	2.3	0.17	0.19	25 ^a

Incubation deployment periods in local time, cloud description, surface DMS concentration (nM), particulate and dissolved DMSP concentrations (nM), nitrate concentration (μM), surface chlorophyll *a* concentration (mg m^{-3}), and mixed layer depth (m) for each incubation. Mixed layer depth was determined as the depth at which potential density exceeded surface potential density by 0.02 kg m^{-3} .

^aTo the bottom.

Chlorophyll *a* analysis was carried out following standard fluorometric procedures using a Turner Designs TD 700 digital fluorometer (Parsons et al., 1984). Nutrient samples were gravity filtered through GF/F filters, stored frozen, and transferred to the Dauphin Island Sea Laboratory for analysis on a Skalar San++ system following standard colorimetric methods (Parsons et al., 1984). For algal pigment analyses, known volumes of seawater were gently vacuum filtered onto GF/F filters. The filters were flash frozen in liquid nitrogen, stored in a -70°C freezer for the duration of the cruise, transported via a dry dewar to the Center for Hydro-Optics and Remote Sensing, and were analyzed following standard HPLC flow injection techniques (Wright et al., 1991). Bacterial production was determined using the tritiated leucine incorporation method (Smith and Azam, 1992).

2.2. Free-floating drifter array

The influence of solar radiation on the rate constants for DMS photolysis and total (photochemical + biological) consumption within the upper water column was measured utilizing a free-floating drifter array. Quartz tubes containing surface seawater were suspended on large grid wire racks held at five fixed depths, ranging from the surface down to 29 m. Exposure depths were adjusted at each station according to water column $a_{\text{CDOM}}(\lambda)$ and UVR attenuation. Temperature differences from the surface to the deepest sample were $<0.35^\circ\text{C}$ at all stations except 14, which

varied by 1.5°C due to the extremely shallow mixed layer. At stations 3 and 4 the surface irradiated samples were held in a flowing water bath on the deck of the ship. These samples potentially experienced slight shading by the ship superstructure, therefore, at station 11 we switched to a floating rack that was attached to the drifter surface buoy. The drifter array was deployed from approximately 10:30–17:30 local time and, except for deployment and retrieval periods, the ship stayed more than 100 m from the array to avoid shading. Three different types of samples were placed in duplicate at each depth on the array: (1) $0.2 \mu\text{m}$ filtered surface seawater amended with tracer levels of ^{35}S -DMS to determine DMS photolysis rates; (2) unfiltered surface seawater amended with tracer levels of ^{35}S -DMS to determine total (photochemical + biological) DMS consumption rates; and (3) unfiltered surface seawater with no tracer amendments to determine post-drifter DMS concentrations, biological DMS consumption rates, and ^3H -leucine incorporation (a measure of bacterial biomass production). The quartz tubes used were $\sim 3 \text{ cm}$ in diameter, and sealed with either solid PFA Teflon stoppers (Kieber et al., 1997) or with Teflon lined gray butyl rubber stoppers and crimp caps. Dark samples were wrapped in aluminum foil and stored in a dark circulating surface water bath.

2.3. Deckboard incubations

In parallel with the drifter deployments, deckboard incubations utilizing optical, long-pass filters

were performed at 10 stations to assess the wavelength dependence of DMS photolysis. Duplicate quartz tubes filled with 0.2 μm filtered seawater and amended with ^{35}S -DMS tracer were exposed to different spectral irradiances with nominal wavelength cut-offs at 50% transmission of 295, 309, 318, 328, 341, 370, 382, and 400 nm. For comparison, additional quartz tubes were exposed to full sunlight or wrapped in aluminum foil as dark controls. Samples were incubated in shallow baths with circulating surface seawater from the underway system to maintain the in situ seawater temperature. The water baths were painted flat black to minimize any scattered or reflected light.

2.4. DMS analysis

All samples for water column DMS concentrations were immediately drawn from the CTD once it was on board. Sample collection bottles were rinsed three times with seawater and were then allowed to overflow equivalent to approximately one volume. Water column and post-drifter array samples were placed in the dark at in situ temperatures and were processed within 2 h of collection. Concentrations were determined using a modified purge and trap method following Kiene and Service (1991). Briefly, 4 mL of sample was taken up into a glass syringe and gently filtered through a GF/F filter into a sparging tube. Sulfur gases were sparged from the water with a stream of helium and trapped in a loop of Teflon tubing immersed in liquid nitrogen. Trapped gases were analyzed on a Shimadzu GC-14A gas chromatograph (GC) equipped with a flame photometric detector and a Carboxpak B 1% XE, 1.5% H_3PO_4 packed column (Kiene and Hines, 1995). The GC was operated at a column temperature of 100 $^\circ\text{C}$ and a detector temperature of 175 $^\circ\text{C}$. The carrier, sparge, and sweep gases were ultra-high purity helium and calibration was carried out with a permeation system. All samples were analyzed in duplicate, with analytical precision better than 5% for all samples.

2.5. ^{35}S methods

All DMS photolysis and total (photochemical + biological) consumption rate determinations were made with ^{35}S -DMS tracer additions (Kiene and Linn, 2000), an approach that gives identical results with GC-based DMS loss measurements (Toole et al., 2004). After the seawater samples were placed

in quartz tubes, radioactive ^{35}S -DMS tracer was added as a gas (~ 0.1 mL). Tracer additions were typically 1000 dpm mL^{-1} , corresponding to an addition of less than 0.05 nM. These additions were always <10% of the natural DMS concentration and thus did not significantly perturb the natural concentration. Photochemical or biological consumption of DMS results in the conversion of volatile ^{35}S -DMS tracer into non-volatile degradation products (Kiene and Linn, 2000). At the conclusion of the incubations, 1 mL of sample was drawn from each quartz tube to quantify the total amount of ^{35}S -DMS added and 3 mL of sample was sparged for 10 min with high purity nitrogen (100 mL min^{-1}) to strip away the volatile ^{35}S -DMS leaving only the non-volatile degradation products. A 1 mL aliquot of the sparged sample was pipetted into 5 mL of Ecolume scintillation cocktail for enumeration on a scintillation counter (Packard Tri-Carb model 2500 TR). All samples were analyzed in duplicate, with analytical precision better than 6%.

The fraction of DMS consumed was quantified as the dpm of non-volatile radioactive sulfur products divided by the total dpm of ^{35}S -DMS added. Photochemical and total consumption rate constants were calculated assuming first-order kinetics, and rates were calculated as the product of rate constants and the initial, pre-exposure DMS concentration (Kieber et al., 1996). At the completion of each incubation, all samples were placed in the dark at in situ temperature for up to 1 h prior to processing. While photolysis ceased, biological DMS consumption continued. As such, biological consumption rates were estimated by calculating the difference between the total consumption and photolysis rates with the incubation time taken as the time interval between initial tracer addition and final analysis. The <1 h additional dark incubation (after light exposure) did not appear to significantly affect results as the magnitude of inhibition of the biological consumption rate constants in the drifter array was similar to that observed in 6–8 h post-drifter dark incubations (see below). Post-drifter biological DMS consumption rate constants were measured by incubating light exposed unfiltered seawater from the retrieved drifter array with tracer ^{35}S -DMS in the dark for a period of 6–8 h (i.e. post-drifter). Rate constants were multiplied by the post-drifter DMS concentration to achieve DMS consumption rates.

2.6. Optical determinations

Vertical profiles of spectral downwelling irradiance ($E_d(z, \lambda)$) and upwelling radiance ($L_u(z, \lambda)$), as well as the time course of $E_d(0^+, \lambda, t)$, were determined using a Satlantic (Halifax, Nova Scotia, Canada) SeaWiFS profiling multi-channel radiometer (SPMR), coupled with a continuously sampling SeaWiFS multi-channel surface reference (SMSR). The SPMR was deployed several times a day in free-fall mode allowing it to sample at a distance of over 10 m from the ship, minimizing effects from ship shadow and instrument tilt (Waters et al., 1990). The SMSR was mounted to the deck and care was taken to avoid shadows or reflected light associated with ship superstructure. To reduce instrument variability due to temperature gradients and fluctuations, the SMSR had a collar of continuously flowing surface seawater. Both sensors sampled 11 wavelengths, nominally 325, 340, 380, 412, 443, 490, 510, 555, 565, 665, and 683 nm, had a sampling rate of approximately 6 Hz, and an approximate bandwidth of 10 nm. All calibrations were carried out by the University of California, Santa Barbara (UCSB) Ocean Optics calibration laboratory and the data were processed using standard procedures (e.g. Siegel et al., 1995).

Incident $E_d(0^+, \lambda, t)$ in the UV was also measured every 30 s via a GUV-511C deck mounted cosine-corrected radiometer (Biospherical Instrument Inc. (BSI), San Diego, CA). The incident flux was measured at four wavelengths (305, 320, 340, and 380 nm) along with integrated photosynthetically active radiation (PAR, 400–700 nm). The GUV was equipped with active internal heating to eliminate instrument variability due to temperature fluctuations and was calibrated using the average of BSI calibrations and pre- and post-cruise UCSB calibrations, with the exception of the 305 nm channel, which was calibrated solely with the BSI coefficients.

2.7. Integrated light dose at depth

To investigate the impacts of light on the rates of DMS photochemical and biological consumption it is critical to accurately quantify the light dose at each incubation depth. For photochemical or photobiological processes, the quantity of interest is scalar irradiance (i.e. the photon energy reaching each incubation) rather than traditionally measured planar or cosine-weighted irradiance. Planar irra-

diance incorporates directional information but photons possess a fixed amount of energy regardless of the direction they originate from. The conversion is also critical as scalar irradiance incorporates the lower hemisphere, the ‘upward’ traveling photons, which can constitute a significant portion of the total photon flux in oligotrophic waters. The following methods were used to estimate planar and scalar irradiance dose at each drifter array incubation depth.

In the upper water column, light attenuates following a simple exponential decay function:

$$E_d(z, \lambda, t) = E_d(0^-, \lambda, t)e^{-K_d(\lambda)z}, \quad (1)$$

where $E_d(0^-, \lambda)$ is the incident flux propagated through the air–sea interface to just beneath the surface assuming a 2% surface reflection (Austin, 1974), $K_d(\lambda)$ is the spectral diffuse attenuation coefficient (m^{-1}), z is the depth (m), and t is the time. Daily mean $K_d(\lambda)$ attenuation coefficients ($\overline{K_d(\lambda)}$) were derived as the average of individual $K_d(\lambda)$ coefficients determined from each SPMR profile as the slope of log-transformed $E_d(z, \lambda)$ vs. depth. Based on water clarity, the depth interval for this calculation varied from <10 m for UV wavelengths in highly productive waters to 30 m for blue wavelengths in oligotrophic waters. The planar irradiance dose integrated over the incubation period at each depth ($E_d(z, \lambda)$, photons m^{-2}) was determined from the continuous measure of surface flux from the SMSR:

$$E_d(z, \lambda) = \int_{t_0}^{t_f} E_d(0^-, \lambda, t)e^{-\overline{K_d(\lambda)}z} \frac{\lambda}{hc} dt, \quad (2)$$

where t_0 is the incubation start time, t_f is the incubation end time, $E_d(0^-, \lambda, t)$ is the time course of incident irradiance propagated through the sea surface ($\text{W m}^{-2} \text{nm}^{-1}$), h is Planck’s constant, c is the speed of light in a vacuum, and λ/hc converts the photon flux at a given wavelength to energy.

To convert the integrated light determinations from planar (Eq. (2)) to scalar irradiance ($E_o(z, \lambda)$), a geometric correction factor (μ'), derived from a series of HYDROLIGHT (Mobley, 1994) underwater radiative transfer simulations, was applied:

$$E_o(z, \lambda) = E_d(z, \lambda)/\mu'(b/a, \theta_s, \overline{\text{cl}}, \tau). \quad (3)$$

This correction is a function of the wavelength specific backscattering to absorption ratio (b/a), solar zenith angle (θ_s), fractional cloud cover ($\overline{\text{cl}}$), and optical depth (τ) (Nelson, pers. comm.). Solar zenith angle was estimated based on time of day,

latitude, and longitude, fractional cloud cover was estimated from the SMSR time course of incident irradiance vs. theoretical clear sky irradiance, and optical depth was calculated from depth and $K_d(\lambda)$. Total absorption was taken as the sum of absorption by CDOM, pure water, and particles, and total scattering coefficients were derived as a function of chlorophyll concentrations (Morel and Maritorena, 2001; see Toole et al., 2003 for methods). The geometric correction was modified for the deckboard incubations because of the lack of an upward photon flux. Similar HYDROLIGHT radiative transfer simulations indicate that in the deckboard incubator, the correction factor is simply a function of fractional cloud cover, solar zenith angle, and incubation depth and does not depend on the inherent optical properties of the water column.

2.8. DMS sea-air flux

DMS sea-air flux was estimated using a standard flux parameterization incorporating the sea surface DMS concentration and a sea-air exchange rate constant (Nightingale et al., 2000):

$$\begin{aligned} \text{Flux}_{\text{sa}} &= k_w[\text{DMS}] \\ &= (0.22U^2 + 0.33U)(Sc/600)^{-1/2}[\text{DMS}], \quad (4) \end{aligned}$$

where Flux_{sa} is the atmospheric ventilation rate of DMS ($\mu\text{mol m}^{-2} \text{d}^{-1}$), k_w represents the gas exchange coefficient (cm h^{-1}), $[\text{DMS}]$ is the concentration of DMS at the sea surface (nM), U is the wind speed (13.5 m collection height, m s^{-1}), and Sc is the dimensionless Schmidt number which encapsulates physical and chemical properties including the diffusivity of DMS (Saltzman et al., 1993). There are a wide variety of flux parameterizations available that can vary by as much as a factor of three at low to moderate wind speeds ($<15 \text{ m s}^{-1}$) suggesting uncertainties on the order of $\pm 150\%$. The Nightingale et al. (2000) parameterization was chosen however because it is a reasonable average of the flux parameterizations available in the literature. Daily ventilation estimates were calculated from Eq. (4) based on the time course of surface seawater temperature from the underway system (intake at 3.6 m), the time course of wind speed from the mast mounted anemometer, and the surface DMS concentration from the morning CTD cast.

2.9. Interpolating measured rate constants with depth

Measured DMS photolysis rate constants were interpolated with depth utilizing the best-fit exponential decay function and the location and day of year derived photoperiod. Post-drifter biological consumption rate constants were linearly interpolated to the deepest incubation depth and were then extrapolated to the dark consumption rate constant at the 1% light level for total UVR. Linear interpolation was utilized because of the poor correlation between UVR dose and biological consumption rates ($r^2 = 0.11$) and the often non-exponential vertical profiles (see below). Although diel variations are expected, post-drifter rate constants were utilized and assumed constant over the 24-h light-dark cycle because they reflect the combined effects of inhibition due to light exposure and dark recovery ($\sim 6\text{--}8 \text{ h}$ incubation each). It should be noted that the drifter array biological consumption rate constants were utilized for station 3 as post-drifter rates were unavailable. For comparison purposes, all rate constants were converted to rates based on the initially sampled morning profile of DMS concentrations interpolated with depth.

3. Results

3.1. DMS photolysis

Results from the drifter incubations of $0.2 \mu\text{m}$ filtered surface seawater revealed that at surface levels of irradiance, DMS photolysis rate constants ranged from 0.033 to 0.086 h^{-1} in coastal and shelf waters and from 0.026 to 0.029 h^{-1} in oceanic waters. These pseudo-first-order DMS photolysis rate constants decreased exponentially with increasing exposure depth (Fig. 2). Rate constants at the coastal and shelf stations (stations 3, 4, and 15) attenuated more rapidly with exposure depth as compared to oceanic stations (stations 11, 12, and 14). Similar to water column irradiance (Eq. (1)), an attenuation coefficient of photolysis can be calculated based on each individual depth profile as the slope of the log-transformed photolysis rate constants vs. depth. Estimated photolysis attenuation coefficients ranged from 0.30 to 0.36 m^{-1} for productive coastal stations in the Gulf of Maine, 0.17 m^{-1} for coastal North Carolina, and $0.06\text{--}0.09 \text{ m}^{-1}$ for open-ocean stations characterized by low $a_{\text{CDOM}}(\lambda)$ and low mixed layer chlorophyll

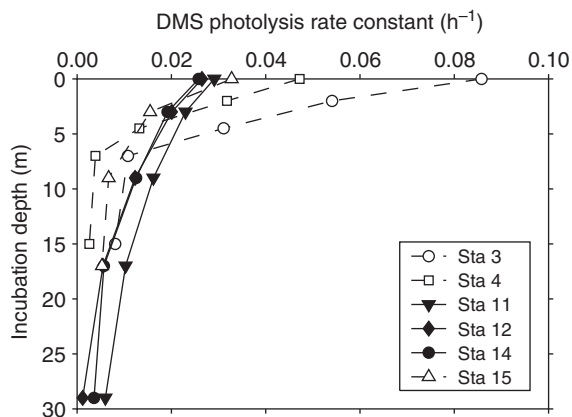


Fig. 2. Vertical profiles of free-floating drifter array-derived DMS photolysis rate constants (h^{-1}) for $0.2\ \mu\text{m}$ filtered surface water incubated at a variety of depths. The coastal and shelf stations (Gulf of Maine (3, 4) and coastal North Carolina (15)) are denoted by dashed lines and open symbols while the Sargasso Sea stations (11, 12, 14) are denoted by solid lines and solid symbols. Variation among duplicate incubations at each depth were $<0.015\ \text{h}^{-1}$ for all samples and $<0.008\ \text{h}^{-1}$ for all but three samples; error bars are omitted for clarity (errors for corresponding rates are shown in Figs. 4 and 5). Incubation times and the corresponding water column properties are noted in Table 1.

biomass (Table 1). Photolysis attenuation coefficients correlated well with CDOM absorption coefficients ($a_{\text{CDOM}}(300)$, $r^2 = 0.95$), which primarily mediate the attenuation, and thus availability, of UVR at depth (Nelson and Siegel, 2002).

At all stations, photolysis rate constants obtained from deckboard incubations were highest in samples exposed to the full solar spectrum and decreased as shorter wavelengths were removed with various long-pass optical filters (see Fig. 3 for example). No statistical differences were found between samples incubated under UV-opaque Lexan (blocks $\lambda < 400\ \text{nm}$) and samples incubated in the dark, confirming that UV wavelengths were responsible for DMS photolysis (e.g. Toole et al., 2003; Bouillon and Miller, 2004). Photolysis rate constants in the full spectrum samples ranged from 0.021 to $0.075\ \text{h}^{-1}$ and were slightly, but consistently, lower than the drifter array surface photolysis rate constants ($r^2 = 0.98$, $n = 6$, slope = 0.80) likely because of the combination of a lack of an upward photon flux and shading from the incubator walls. Based on differences between light treatments, maximum photolysis rates at surface levels of irradiance were observed in the UV-A ($320\text{--}400\ \text{nm}$) spectral region, accounting for a mean of $72.7 \pm 4.9\%$ of the total DMS photolysis in nine

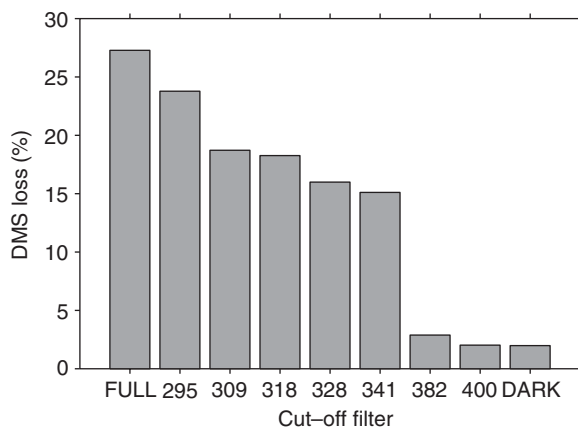


Fig. 3. Percentage of initial DMS photolyzed under a variety of long-pass filters during a 6.6 h incubation (10:39–17:15 local time) of $0.2\ \mu\text{m}$ filtered surface seawater collected at station 4. Nominal filter cut-off wavelength is calculated as the wavelength where transmission is 50% of maximum transmission. The optical cut-offs were created using UVR transparent acrylic for 295 nm (UVT, Poretics Plastic), Schott glass filters for 309 nm (WG305), Schott glass filters for 318 nm (WG320), UVT + .005" Mylar for 328 nm, UVT + .007" Mylar for 341 nm, Chemcast cell cast acrylic for 382 nm, and Lexan for 400 nm. FULL indicates no cut-off filter and DARK indicates samples wrapped in aluminum foil and incubated in a dark circulating surface water bath.

experiments (Table 2). In contrast, UV-B wavelengths ($280\text{--}320\ \text{nm}$) were responsible for $20.0\text{--}37.9\%$ (mean $27.3 \pm 4.9\%$) of the total photolysis (Table 2).

3.2. Photolysis vs. total DMS consumption

In addition to the photolysis rate constants obtained in $0.2\ \mu\text{m}$ filtered seawater, total DMS consumption rate constants and rates (photochemical + biological) were obtained by incubating tracer ^{35}S -DMS in unfiltered surface seawater samples on the free-floating drifter array (Figs. 4A–C and 5A–C). Although surface photolysis rate constants were lower in oceanic waters (Fig. 2), photochemical and total DMS consumption rates were higher at these stations as a result of systematically higher surface DMS concentrations (Table 1). Total DMS consumption rate constants, and rates, were largest at surface levels of irradiation and generally decreased with increasing incubation depth indicating the dominance of photolysis (see Fig. 6 for example). At stations 4 and 15 however, total DMS consumption rates increased slightly or remained constant at depths deeper than $\sim 10\ \text{m}$ suggesting that other non-photochemical processes made significant

Table 2
DMS photolysis factors

Station	SST	$a_{CDOM}(300)$	DOC concentration	% contribution by UV-A	% contribution by UV-B	# Light treatments
3	5.3	0.779	70.21	75.6	24.4	9
4	4.6	0.821	68.15	72.5	27.5	9
6	15.0	0.410	66.78	62.1	37.9	8
8	19.5	0.157	61.91	72.6	27.4	8
11	21.0	0.193	65.40	72.7	27.3	6
12	21.2	0.172	65.63	70.4	29.6	6
13	21.6	0.215	65.00	80.0	20.0	9
14	22.5	0.196	66.17	72.7	27.3	8
15	22.1	0.399	71.09	75.8	24.2	7

At each station ancillary data were monitored which impact DMS photolysis rates. SST was determined from the early morning CTD cast and $a_{CDOM}(300)$ (m^{-1}) and DOC concentration ($\mu mol L^{-1}$) were determined utilizing pre-incubated surface samples. The percent contributions of photolysis in the UV-A and UV-B wavelength regions to total photolysis were estimated from the deck-box photolysis rates. The number of light treatments is the total number of cut-off filters utilized in the deckboard incubations.

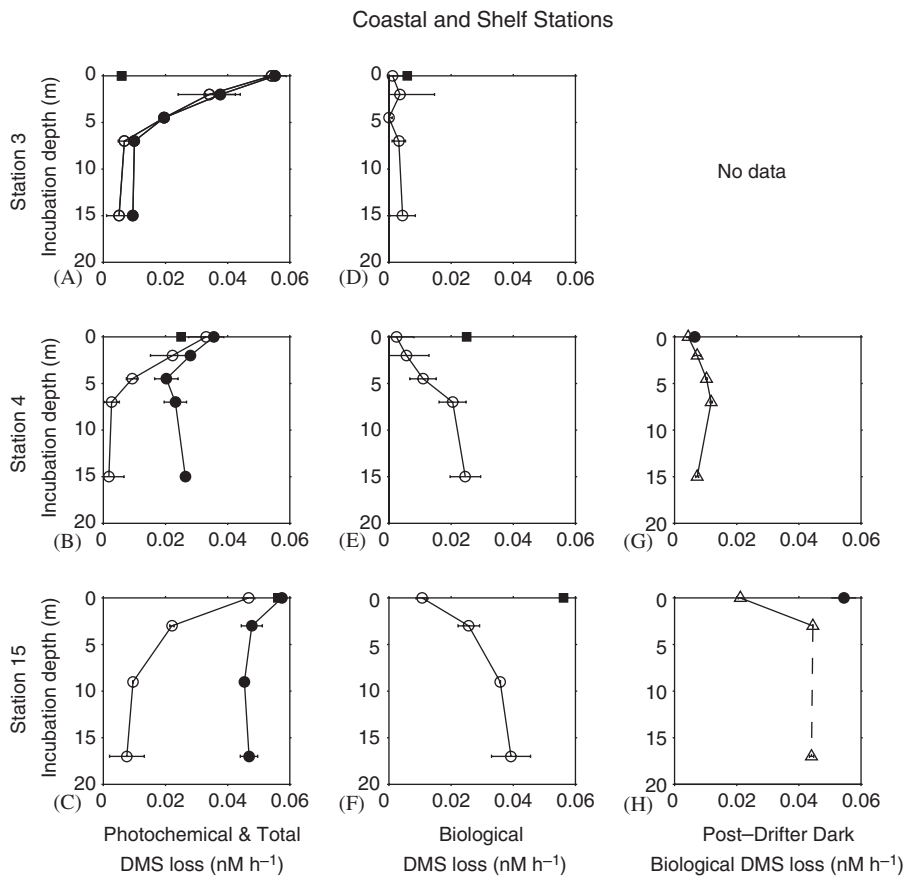


Fig. 4. Effects of incubation depth on photochemical (\circ) and total (\bullet) DMS consumption rates (A–C, $nM h^{-1}$), estimated biological DMS consumption rates (D–F, $nM h^{-1}$, total—photochemical), and post-drifter dark biological DMS consumption rates (G, H, $nM h^{-1}$) \pm standard deviation for surface water incubated on the drifter array at the coastal and shelf stations (3, 4, 15). Corresponding dark rates are denoted with the solid square in panels A–F and the solid circles in panels G–H. All samples were collected at the surface and are shown in terms of incubation depth.

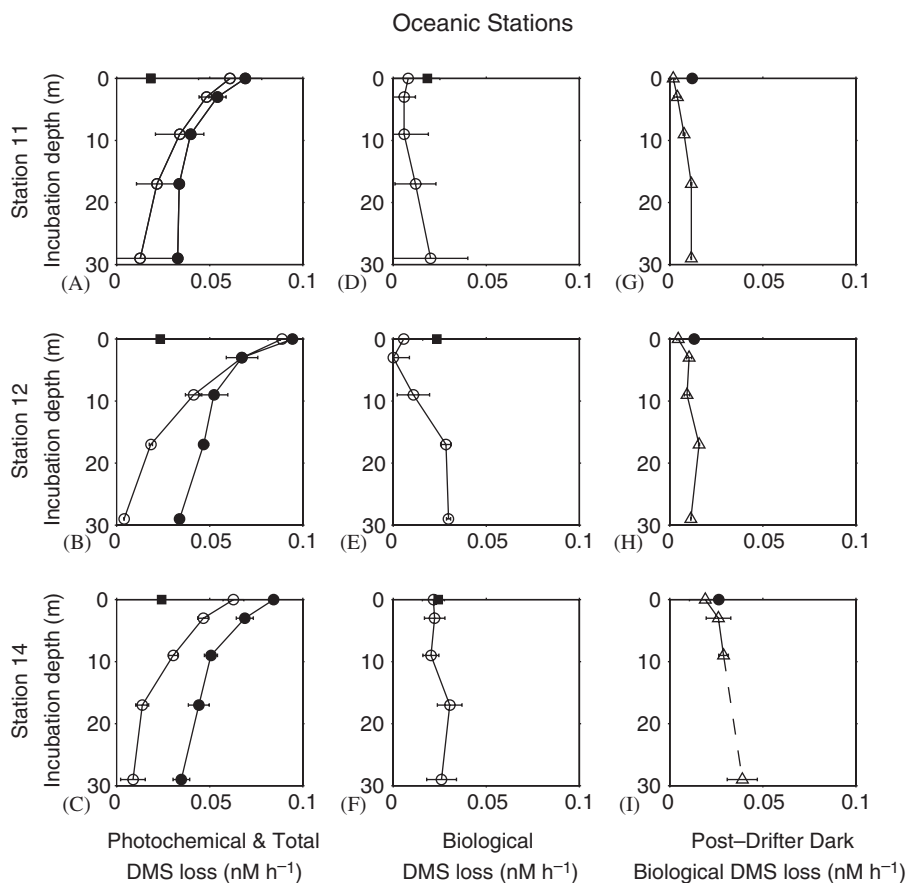


Fig. 5. Effects of incubation depth on photochemical (\circ) and total (\bullet) DMS consumption rates (A–C, nM h^{-1}), estimated biological DMS consumption rates (D–F, nM h^{-1} , total—photochemical), and post-drifter dark biological DMS consumption rates (G–I, nM h^{-1}) \pm standard deviation for surface water incubated on the drifter array at the open-ocean stations (11, 12, 14). Corresponding dark rates are denoted with the solid square in panels A–F and the solid circles in panels G–I. All samples were collected at the surface and are shown in terms of incubation depth. Note the x- and y- axis scale change as compared to Fig. 4.

contributions. At station 3 in the Gulf of Maine, and at station 12 in the Sargasso Sea, the total and photochemical loss rates were nearly identical in samples exposed in the upper 10 m, indicating a very small biological contribution to DMS losses (see below). This small biological loss at station 3 is also reflected in the low rate obtained in dark incubated whole water samples (Fig. 4A). For all other stations and exposure depths, total DMS consumption was greater than photolysis, suggesting contributions from biological processes. While it is possible that the larger rates in the unfiltered samples could have been due to particle-assisted photolysis, or an increase in photolysis due to biological exudates, the observed patterns with depth do not support this. At most stations the difference between total loss rates and photochemical loss rates were small near the surface (upper

10 m) and increased with deeper exposure depth, arguing against a contribution by photolysis to the difference in rates.

3.3. Biological consumption of DMS

At surface levels of irradiance, estimated biological DMS consumption rates ranged from 0.002 to 0.022 nM h^{-1} , while corresponding dark consumption rates ranged from 0.006 to 0.056 nM h^{-1} indicating significant inhibition at shallower exposure depths (Figs. 4D–F and 5D–F). Samples exposed at deeper depths were characterized by biological DMS consumption rates similar to those obtained in the dark. UV inhibition, calculated as the percent reduction in biological consumption rates when compared to dark consumption rates, ranged from a maximum of nearly 90% inhibition

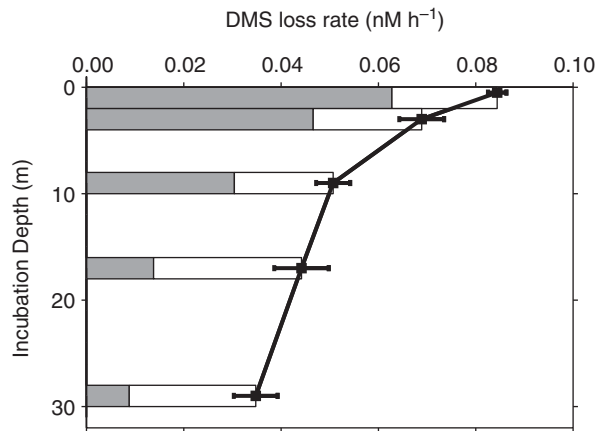


Fig. 6. Representative example of total (photochemical+ biological) DMS loss in surface seawater from station 14 as a function of in situ incubation depth (thick black line). The contributions of photolysis and estimated biological consumption to each determination are indicated by the horizontal bars (gray, photolysis; white, biological consumption). Error bars denote ± 1 standard deviation for the measured, total DMS loss.

at surface levels of irradiance to less than zero ($> 120\%$ of dark values) at deeper exposure depths. This inhibition varied with location, with more productive stations characterized by biological populations more sensitive (i.e. higher inhibition) to surface level doses of UVR ($84 \pm 5\%$ inhibition at the surface for coastal and shelf stations vs. $47 \pm 33\%$ inhibition at the surface for open-ocean stations).

The UVR-induced inhibition of biological DMS consumption at shallow depths was also revealed in post-drifter, dark incubations. Samples irradiated near the surface generally had lower post-drifter consumption rates than those exposed at depth reflecting continued inhibition of dark biological DMS consumption in the dark. While the exposure and depth patterns were generally similar for the two types of biological DMS consumption rates we measured, they were not identical. This is not surprising because the estimated biological consumption rates were obtained in the light during the drifter deployment, and thus reflect consumption rates that are affected by accumulating cellular damage by light. In contrast, the post-drifter, dark incubations are a combination of the end result of light inhibition that occurred during the drifter deployment followed by biological recovery that may have occurred during the 6–8 h dark incubations. The light-inhibited post-drifter DMS consumption patterns were similar to those obtained

for post-drifter ^3H -leucine incorporation, a measure of bacterial biomass production (data not shown).

The dependence of biological DMS consumption rates on UVR exposure at each drifter station was calculated as the slope of the log-transformed consumption rate constants vs. depth (functional form similar to Eq. (1)). While the biological consumption rate constant profiles are noisier than corresponding photolysis rate constant profiles and less suited to exponential fits, this calculation allows for a first-order assessment of the sensitivity of the biological communities to UVR and the depth range over which UV inhibition occurred. Estimated attenuation coefficients were variable: -0.10 m^{-1} for station 3 in the Gulf of Maine, -0.30 m^{-1} for station 4 in the Gulf of Maine, -0.12 m^{-1} for coastal North Carolina, and -0.01 to -0.06 m^{-1} for open-ocean stations. The significant relationship between $a_{\text{CDOM}}(300)$ and these attenuation coefficients ($r^2 = 0.64$) supports the supposition that the availability of UVR impacts the degree of inhibition of biological DMS consumption.

For comparison to the light exposed samples, we also measured the biological DMS consumption rate constants obtained from morning depth profiles (water collected at each depth and incubated with ^{35}S -DMS in the dark) at each station (Fig. 7). These in situ profiles also indicate lower rate constants in the surface mixed layer as compared to deeper depths, especially at the oceanic stations where light penetration was greatest. Additionally, the rate constants were relatively uniform within the surface mixed layer supporting the assumption of homogeneity of the microbial community over this depth range with respect to DMS consumption. Some of the increase with depth may be attributed to different water mass layers or vertical structure in the microbial composition, but the pattern is consistent with light-driven inhibition of biological DMS consumption in surface waters. These rates suggest that the biological populations responsible for DMS consumption are slow to recover from UV inhibition as the samples were collected after the full night period and were then held in the dark for an additional 6–8 h during incubation.

3.4. DMS loss process comparison with depth

To assess the variability in DMS loss processes as a function of depth, the contributions of depth-integrated photolysis and biological consumption

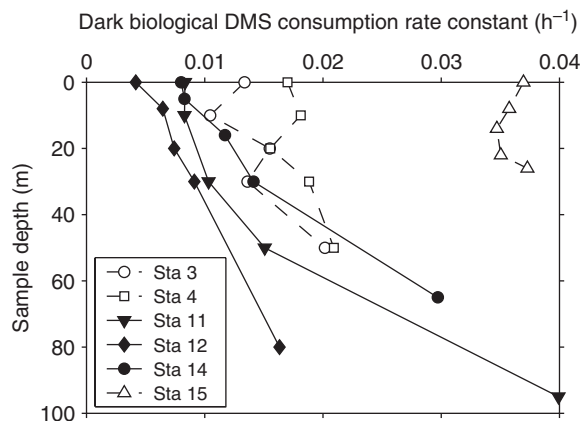


Fig. 7. Depth profiles of dark biological DMS consumption rate constants (h^{-1}) obtained from morning 06:00 CTD casts. The coastal and shelf stations (Gulf of Maine (3, 4) and coastal North Carolina (15)) are denoted by dashed lines and open symbols while the Sargasso Sea stations (11, 12, 15) are denoted by solid lines and solid symbols. Variation among duplicate incubations at each depth were $<0.003 \text{ h}^{-1}$ in all cases; error bars are omitted for clarity. Unlike the drifter array data, these data represent dark biological consumption rate constants from seawater samples collected at the indicated depth.

were compared to estimates of sea-air ventilation over a variety of integrated depth horizons from the surface to the base of the mixed layer, 1 m, 15 m, and the 1% light level for 325 nm (approximating the maximum depth of UV-B penetration). These calculations assume that the DMS photolysis and biological consumption rates obtained by incubating surface water at different depths in the mixed layer are representative of the mixed layer (see Section 3.3 for morning profiles). Clearly, this assumption will break down at depths below that of the mixed layer or if there is defined vertical structure in the microbial community with respect to DMS cycling.

The most relevant depth horizon to consider for DMS cycling is that of the mixed layer, as sources and sinks of DMS to this layer will govern the steady-state concentration and hence flux of DMS to the atmosphere. Estimated total (photochemical + biological + sea-air) DMS turnover rates in the mixed layer ranged from 8.1 to $44.5 \mu\text{mol m}^{-2} \text{d}^{-1}$ with turnover times ranging from 0.87 to 3.2 d (Fig. 8). Relative to this total, estimated daily sea-air DMS flux rates were small, ranging from $0.39 \mu\text{mol m}^{-2} \text{d}^{-1}$ at station 3, which exhibited low SSTs (5.6°C), lower wind speeds ($2.3\text{--}6.4 \text{ m s}^{-1}$), and low surface DMS concentrations (0.63 nM), to

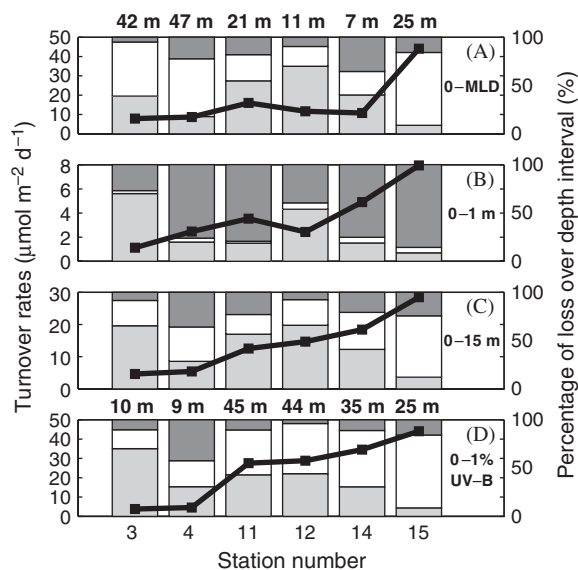


Fig. 8. Percent contribution of sea-air flux (dark gray), biological consumption (white), and photolysis (light gray) processes to total DMS loss rates over a variety of depth intervals. The vertical bars correspond to 100% of the loss rate and the depth-integrated DMS turnover rates at each station are overlaid as the solid black line. For reference, the depth of the mixed layer (m) and the 1% light level for 325 nm (m) are noted for each station at the top of panels A and D, respectively.

$6.93 \mu\text{mol m}^{-2} \text{d}^{-1}$ at station 15, which exhibited relatively high SSTs (22.1°C), relatively high surface DMS concentrations (1.43 nM), and the highest observed wind speeds ($7.4\text{--}12.2 \text{ m s}^{-1}$). At the open-ocean Sargasso Sea sites, characterized by shallow mixed layer depths (Table 1), photolysis processes dominated with biological consumption and sea-air flux accounting for only $24.0 \pm 3.3\%$ and $21.0 \pm 13.2\%$ of the total DMS loss, respectively (Fig. 8A, stations 11, 12, and 14). In contrast, at more productive sites in the Gulf of Maine and coastal North Carolina where deeper mixed layer depths were observed, biological consumption dominated DMS loss, contributing 54.0–74.4% of the total (Fig. 8A, stations 3, 4, and 15). Thus for a given light regime, as the mixed layer depth deepens, the importance of the sea-air flux and depth-integrated photolysis decreases, whereas the depth-integrated biological consumption rate increases.

Since mixed layer depth can respond rapidly to synoptic meteorological forcing, we also calculated the contributions of the three primary loss terms over several depth intervals from the surface to 1 m, 15 m, and to the 1% light level for UV-B. Similar to

previous findings (e.g. Kieber et al., 1996) biological consumption did not make a significant contribution to the total DMS removal in the upper 1 m of the water column, with photolysis and sea-air exchange dominating the total DMS turnover (Fig. 8B). Atmospheric ventilation accounted for less than 50% of the total DMS loss and photolysis dominated at station 3, which exhibited low SSTs and wind speeds. A similar situation was observed at station 12 where wind speeds were extremely low, $0.9\text{--}4.3\text{ m s}^{-1}$. Stations 4, 11, 14, and 15 were characterized by higher wind speeds and thus atmospheric ventilation was the dominant loss mechanism for the upper 1 m.

Over the 0–15 m depth interval, sea-air ventilation made a smaller contribution to total loss, whereas the contribution of biological consumption increased (Fig. 8C). This is consistent with sea-air flux processes acting only at the surface and the gradients with depth of photolysis and biological consumption rates modulated by the attenuation of UVR. The greater the attenuation of UVR, the smaller the depth range over which photolysis will make a significant contribution to total DMS loss, leading to dominance of biological processes at depth.

It is interesting to note that the contributions of the various loss processes at stations 3 and 12 are strikingly similar to each other, despite the fact that water mass characteristics differed considerably at these two stations (Table 1). While the percent contributions are similar, the total, photochemical, and biological consumption turnover rates were approximately 2.5 times higher at station 12 because of the larger in situ DMS concentration. This indicates that there can be a balancing effect between decreased incident light flux, high $a_{\text{CDOM}}(\lambda)$, and low biological consumption rates as observed at station 3. At the same time, when results from station 3 are compared to those from station 4, a two-fold difference in the contribution of the integrated biological DMS consumption was observed despite the fact that both stations had nearly identical hydrographic and optical characteristics (Table 1). The primary difference between the stations was the clear sky at station 3, allowing a larger UV dose, compared to overcast conditions at station 4. The combination of reduced UV flux and the more active biological population greatly reduced the importance of photolysis as a removal mechanism at station 4.

When removal rates were integrated from the surface to the 1% light level for 325 nm, with the

exception of station 3, photolysis represented <50% of the total DMS loss (Fig. 8D). The contribution of photolysis to the total may be even somewhat lower at these stations however. Our measured biological DMS consumption rates may underestimate the true biological contribution due to the lack of mixing in the array samples and the resulting potential overestimation of UV-induced inhibition of DMS consumption.

3.5. Changes in DMS concentrations as a function of light dose

Because of the complex and dynamic nature of DMS production and loss processes, it is crucial to assess how changes in the concentration of DMS will vary as a function of UVR exposure. During the drifter array incubations, DMS concentrations in the quartz tubes with unfiltered water increased at some stations (stations 4 and 14), decreased at others (stations 11 and 12), or had variable changes (stations 3 and 15), and overall, there was no significant trend with UV dose (Fig. 9A). This contrasts with findings from the Sargasso Sea which indicated that mean mixed layer DMS concentrations increased with increasing mean mixed layer UVR exposure on seasonal time scales (Toole and Siegel, 2004). These contrasting results are likely due to differences in the measurement frequency, as the Dacey et al. (1998) DMS time-series data set used in the Toole and Siegel (2004) analysis had a sampling frequency of 2 weeks whereas this study monitored DMS concentration changes over 6–8 h. It is likely that high levels of day-to-day variability in DMS production and loss processes (e.g. Simó and Pedrós-Alió, 1999b) resulting from inhibition and acclimation of biological populations on short time scales, as observed in this study, are superimposed on a larger trend associated with seasonal UVR fluxes.

In contrast to the relatively small observed concentration changes in DMS, total (photochemical + biological) DMS loss rates increased linearly as a function of cumulative UVR dose ($r^2 = 0.69$, Fig. 9B). The fact that DMS consumption rates were significantly higher in the light exposed samples, and yet the final concentrations did not display a corresponding pattern, indicates that an equivalent light-mediated biological DMS production ranging up to 0.35 nM h^{-1} (based on the assumption of mass balance) must have occurred. This positive relationship is consistent with the net

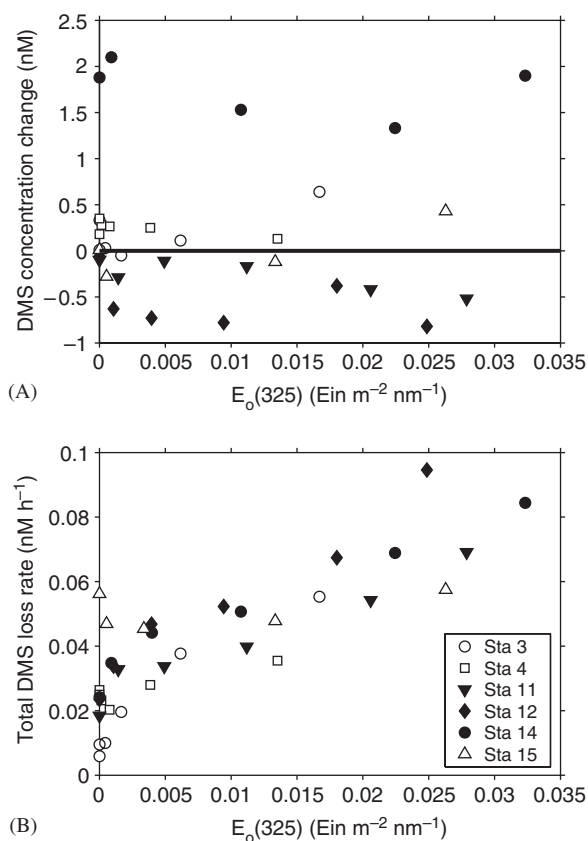


Fig. 9. (A) Absolute DMS concentration change (nM) and (B) total DMS loss rates (nM h^{-1} , photochemical + biological) as a function of scalar irradiance dose at 325 nm over the duration of the drifter array incubations. The symbols are the same in both panels.

biological production of DMS in response to UVR suggested by Toole and Siegel (2004). As biological DMS consumption was clearly inhibited by UVR (Figs. 4 and 5), the increased biological DMS production could have resulted from either an increase in DMSP and DMS production or release by phytoplankton in response to photo-oxidative stress (Sunda et al., 2002), changes in microzooplankton grazing during incubations, or a change in the bacterial processing of dissolved DMSP.

4. Discussion

The in situ irradiation approach provides the first direct observations of how DMS photolysis and biological consumption rates vary as a function of natural light penetration in the upper ocean. In particular, the free-floating drifter array results indicate strong potential for UVR-induced inhibi-

tion of near surface biological DMS consumption. At surface levels of irradiation, surface seawater samples displayed inhibition ranging from $85 \pm 5\%$ in coastal and shelf regions to $47 \pm 33\%$ at open-ocean stations. The higher inhibition in coastal areas may reflect microbial populations that are less acclimated to high UV doses because of prevailing deeper mixing conditions and relatively high CDOM absorption of UVR. Conversely, microbial populations in clear, oligotrophic waters routinely experience high UVR doses throughout the mixed layer; therefore, these populations are likely acclimated to UVR. In this study, the oligotrophic stations were characterized by shallow ($<21\text{ m}$) mixed layer depths and low $a_{\text{CDOM}}(\lambda)$; therefore, the initially sampled microbial communities may have already been inhibited from the high daily doses and cumulative exposure of UV-B. At the Sargasso Sea stations, biological DMS consumption rates in the light-exposed samples were greater than dark consumption rates at incubation depths greater than $\sim 20\text{ m}$ (Fig. 5). Past studies indicate that UV-A in the absence of UV-B induces photoenzymatic repair of DNA (e.g. Herndl et al., 1993, 1997). At a depth of 15 m, greater than 85% of the surface UV-B radiation had been attenuated, while $\sim 50\%$ of UV-A remained. Thus, UV-A-induced cell repair or another UV-A or PAR mediated process may have occurred, stimulating an increase in DMS consumption rates and bacterial production rates.

Because the drifter array held samples at fixed depths, thereby eliminating natural vertical mixing processes, the observed light-driven inhibition of DMS consumption is likely an upper limit of expected biological effects. The observed vertical profiles should be fairly accurate representations for calm days however, such as station 12 when wind speed varied from 0.95 to 4.30 m s^{-1} (mean $2.4 \pm 0.6\text{ m s}^{-1}$). The morning profiles of in situ DMS biological consumption rates reflect the combined effects of vertical mixing and nighttime recovery of microbes, yet they still indicate inhibition in the upper water column (Fig. 7). While little is known about the response of biological DMS consumption to UV light dose, it is known that other phytoplankton and bacterial responses can be non-linear and vary as a complex function of cumulative light dose, the temporal pattern of light exposure, mixing depth, and mixing rate (e.g. Huot et al., 2000; Neale et al., 1998). UV-induced inhibition is superimposed on a high degree of natural variability among sampling sites in the dark

biological DMS consumption rates. While drifter array biological DMS consumption rates were clearly influenced by cumulative UVR dose (Figs. 4 and 5) the correlation was quite poor ($r^2 = 0.11$). This result reinforces the large spatial and temporal variability in biological DMS consumption rates expected to result from variations in bacterial community composition, bacterial carbon and sulfur demand, dissolved organic material quality and quantity, and sensitivity to and recovery time from UVR exposure (e.g. Arrieta et al., 2000; Malmstrom et al., 2004; Slezak et al., 2001; Zubkov et al., 2002).

In contrast to its biological consumption, the drifter array results indicate that DMS photolysis occurred at substantial rates in the upper-mixed layer, decreasing exponentially with increasing incubation depth in accordance with the attenuation of UVR. Deckboard polychromatic irradiations showed the same trend, with no photolysis observed at wavelengths longer than 400 nm. Because of this, >95% of DMS photolysis occurred within the upper 20 m at the coastal and shelf sites, while 66–83% of DMS photolysis occurred within the same depth range at open-ocean, oligotrophic sites. The spectral partitioning observed in the deckboard incubations between photolysis by UV-B and UV-A wavelengths will also serve to modulate the depth horizon over which significant DMS photolysis occurs. In the oligotrophic, open-ocean regions of the Sargasso Sea, DMS photolysis rates asymptoted to near zero at ~ 30 m ($K_d(\text{photolysis})$ $0.06\text{--}0.09\text{ m}^{-1}$) whereas this occurred within the upper 15 m ($K_d(\text{photolysis})$ $0.17\text{--}0.36\text{ m}^{-1}$) at more productive coastal and shelf sites. The maximum depth horizon for DMS photolysis will ultimately vary as a function of the wavelength specific attenuation of solar UVR (e.g. Toole et al., 2003). This depth dependence further confirms the dominant role of UVR in driving DMS photolysis (e.g. Toole et al., 2003, 2004) and provides limits for the depth range over which photolysis processes will be significant.

Overall, the biophysical factors that control vertical mixing, and thus UV exposure dose, have opposite effects on DMS photolysis and biological DMS consumption. At surface levels of irradiance, DMS photolysis rate constants ranged from 2 to 19 times those of biological consumption, decreasing in contribution with increasing incubation depth (Fig. 6). Stations with higher $a_{\text{CDOM}}(\lambda)$ were characterized by a more rapid decrease in this ratio

with depth, consistent with the more rapid attenuation of UVR. At each station, the vertical profiles of DMS photolysis and biological consumption rate constants reached an equivalence point in the upper water column, shallower than the 1% light level for 325 nm, indicating that as photolysis decreases because of the attenuation of UVR, biological consumption increases in parallel due to decreased inhibition. Additionally, the biological DMS consumption attenuation coefficients were consistently lower than the photolysis attenuation coefficients indicating that inhibition of biological consumption was a weaker function of UVR than photolysis.

Mixing depth, mixing rate, and the absorption of photons by CDOM impact the dose of solar radiation experienced by organisms (e.g. Denman and Gargett, 1983) suggesting a role for these physical factors in the biogeochemical cycling of DMS in the upper ocean. Many open-ocean regions such as the Sargasso Sea have a regular water column progression beginning with the onset of warming in the spring, leading to a well stratified water column, with a shallow mixed layer in the summer, that progressively deepens in the fall via convective overturn to deep wintertime mixed layer depths (Steinberg et al., 2001). This physical progression is mirrored in the annual CDOM cycle characterized by maximum absorption in surface waters in the winter and spring associated with entrainment of water from depth and minimum absorption coefficients in the summer due to photobleaching processes (Nelson et al., 1998). The magnitude of seasonal variations in $a_{\text{CDOM}}(\lambda)$ and vertical attenuation coefficients at any given open-ocean location will likely be less than those observed in this study, which compared widely different geographic locations, but results from the current study can be considered representative of seasonal end members. For example, the physical and optical patterns observed at the Gulf of Maine stations 3 and 4 are representative of typical winter and spring conditions characterized by higher $a_{\text{CDOM}}(\lambda)$ and deeper mixing. During this time, the relatively high $a_{\text{CDOM}}(\lambda)$ is balanced by reduced incident UV flux, low in situ DMS concentrations, and low temperatures, producing relatively low surface photolysis rates as compared to summertime rates. Additionally, the depth of the mixed layer is often deeper than the depth over which the majority of UVR is absorbed and thus, total photolysis is simply a function of available radiation, which is 2–3 times lower seasonally in temperate latitudes

(Lubin et al., 1998). Similar to the coastal and shelf stations, depth-integrated biological DMS consumption rates are likely to be a dominant loss process in the winter and spring in open-ocean stations because of deep mixing, reduced inhibition of biological DMS consumption, and the fact that much of the mixed layer water column is effectively dark to UV radiation. This is not universal, however, as high nutrient low chlorophyll Antarctic waters demonstrated a dominance of photochemical loss processes in the spring (see Toole et al., 2004).

In contrast to the winter and spring, typical summer conditions are characterized by higher DMS concentrations, higher temperatures, larger incident UV fluxes, shallow mixed layers, and lower $a_{\text{CDOM}}(\lambda)$ resulting in large UV doses in the mixed layer. This combination of factors results in increased surface photolysis rates, which attenuate more gradually with depth, producing a mixed layer DMS consumption profile dominated by photolysis. Clearly, the dominant loss process will vary on a variety of time scales from inter-day to seasonal (e.g. Simó and Pedrós-Alió, 1999b; Toole and Siegel, 2004) but in open-ocean environments, the UVR flux and mixed layer depth covary seasonally suggesting a seasonality to the dominant DMS loss process.

The results from this study confirm that total DMS loss is a complicated balance between upper water column UVR attenuation, the physiological status of the biological assemblage, and physical factors such as mixed layer depth, wind speed, and temperature overlaid on the synoptic variability expected for sea-air ventilation. We have shown that while UVR dose increases DMS photolysis, it can also significantly inhibit biological DMS consumption to depths of 20 m at open-ocean sites. These effects are not offsetting however as profiles of total (photochemical + biological) DMS loss derived from surface water incubated within the upper column were consistently largest at the surface. DMS photolysis and biological consumption, in conjunction with a possible light-driven DMS production process, combined to produce small net changes in DMS concentrations in the samples we studied however (Fig. 9; see also Toole and Siegel, 2004) suggesting that for a more complete understanding of DMS biogeochemical cycling, UVR needs to be quantified in future field and laboratory studies and explicitly included in modeling efforts. To accurately parameterize biological DMS consumption for inclusion in modeling studies, further work is needed to assess the non-

linear UV responses and the varying time scales and forcing factors for inhibition and recovery processes. Our observations of the inhibition of biological DMS consumption rates suggest that shipboard or laboratory incubations, which are traditionally carried out in the dark (e.g. Kiene and Bates, 1990; Kieber et al., 1996; Simó and Pedrós-Alió, 1999b), could significantly overestimate true in situ values in surface waters, or miss light-induced DMS production at deeper depths, thereby adversely affecting modeling studies.

Our results demonstrate that DMS removal rates are strongly influenced by the penetration of UVR, the relative sensitivities of various DMS production and loss terms to UVR, and the depth of the water column constituting the well-mixed layer. As levels of stratospheric ozone continue to change it is crucial to assess how the resulting changes in UV-B radiation will impact not only upper-ocean biogeochemical cycling of DMS, and other climatically relevant trace gases, but also the associated feedback systems. Understanding the role of UVR and mixed layer depth is critical to determining if the sulfur cycle will ultimately display the negative feedback requisite to the cloud-albedo hypothesis.

Acknowledgements

This work was supported by the National Science Foundation (grants OCE-9907471, OCE-0221106, OPP-0230499, and OPP-0221748) and NASA SIMBIOS (NAS5-00200). Any opinions, findings, conclusions, or recommendations expressed in this paper are those of the authors and do not necessarily reflect the views of the National Science Foundation. DAT was supported by a NASA Earth System Science Fellowship. The authors gratefully acknowledge Craig Carlson and his laboratory for DOC analyses, Dave Menzies for calibration and general assistance with the SPMR and SMSR, Paul Ricchiazzi and Catherine Gautier for use of the GUV, Norm Nelson for advice with the optical conversions, Mary-Anne Rouse, Boon Harada, Jody Bruton, Rex Malmstrom, and Allison Buchan for assistance with data collection, and the captain and crew of the R/V *Oceanus* for technical assistance.

References

- Andreae, M.O., Crutzen, P.J., 1997. Atmospheric aerosols: biogeochemical sources and role in atmospheric chemistry. *Science* 276, 1052–1058.

- Arrieta, J.M., Weinbauer, M.G., Herndl, G.J., 2000. Interspecific variability in sensitivity to UV radiation and subsequent recovery in selected isolates of marine bacteria. *Applied and Environmental Microbiology* 66 (4), 1468–1473.
- Austin, R.W., 1974. Inherent spectral radiance signatures of the ocean surface. In: Duntley, S.W., Austin, R.W., Wilson, W.H., Edgerton, C.F., Moran, S.E. (Eds.), *Ocean Color Analysis*. SIO Technical Reference 74-10. Scripps Institute of Oceanography, La Jolla, CA, pp. 2.1–2.20.
- Ayers, G.P., Gillett, R.W., 2000. DMS and its oxidation products in the remote marine atmosphere: implications for climate and atmospheric chemistry. *Journal of Sea Research* 43 (3–4), 275–286.
- Bouillon, R., Miller, W.L., 2004. Determination of apparent quantum yield spectra of DMS photo-degradation in an in situ iron-induced Northeast Pacific Ocean bloom. *Geophysical Research Letters* 31, L06310, doi:10.1029/2004GL019536.
- Brimblecombe, P., Shooter, D., 1986. Photo-oxidation of dimethylsulphide in aqueous solution. *Marine Chemistry* 19, 343–353.
- Brugger, A., Slezak, D., Obernosterer, I., Herndl, G.J., 1998. Photolysis of dimethylsulfide in the northern Adriatic Sea: dependence on substrate concentration, irradiance and DOC concentration. *Marine Chemistry* 59, 321–331.
- Carlson, C.A., Ducklow, H.W., 1996. Growth of bacterioplankton and consumption of dissolved organic carbon in the Sargasso Sea. *Aquatic Microbial Ecology* 10 (1), 69–85.
- Carlson, C.A., Giovannoni, S.J., Hansell, D.A., Goldberg, S.J., Parsons, R., Otero, M.P., Vergin, K., Wheeler, B.R., 2002. Effect of nutrient amendments on bacterioplankton production, community structure, and DOC utilization in the northwestern Sargasso Sea. *Aquatic Microbial Ecology* 30, 19–36.
- Charlson, R.J., Lovelock, J.E., Andreae, M.O., Warren, S.G., 1987. Oceanic phytoplankton, atmospheric sulfur, cloud albedo and climate. *Nature* 326, 655–661.
- Charlson, R.J., Schwartz, S.E., Hales, J.M., Cess, R.D., Coackley, J.A., Hansen, J.E., Hofmann, D.J., 2000. Climate forcing by anthropogenic aerosols. *Science* (255), 423–430.
- Dacey, J.W.H., Howse, F.A., Michaels, A.F., Wakeham, S.G., 1998. Temporal variability of dimethylsulfide and dimethylsulfoniopropionate in the Sargasso Sea. *Deep-Sea Research I* 45, 2085–2104.
- Denman, K.L., Gargett, A.E., 1983. Time and space scales of vertical mixing and advection of phytoplankton in the upper ocean. *Limnology and Oceanography* 28, 801–815.
- González, J.M., Simó, R., Massana, R., Covert, J.S., Casamayor, E.O., Pedrós-Alió, C., Moran, M.A., 2000. Bacterial community structure associated with a dimethylsulfoniopropionate producing North Atlantic algal bloom. *Applied and Environmental Microbiology* 66, 4237–4246.
- Green, S.A., Blough, N.V., 1994. Optical absorption and fluorescence properties of chromophoric dissolved organic matter in natural water. *Limnology and Oceanography* 39, 1903–1916.
- Herndl, G.J., Muller-Niklas, G., Frick, J., 1993. Major role of ultraviolet-B in controlling bacterioplankton growth in the surface layer of the ocean. *Nature* 361, 717–719.
- Herndl, G.J., Brugger, A., Hager, S., Kaiser, E., Obernosterer, I., Reitner, B., Slezak, D., 1997. Role of ultraviolet-B radiation on bacterioplankton and the availability of dissolved organic matter. *Plant Ecology* 128, 42–51.
- Huot, Y., Jeffrey, W.H., Davis, R.F., Cullen, J.J., 2000. Damage to DNA in bacterioplankton: a model of damage by ultraviolet radiation and its repair as influenced by vertical mixing. *Photochemistry and Photobiology* 72 (1), 62–74.
- Kieber, D.J., Jiao, J., Kiene, R.P., Bates, T.S., 1996. Impact of dimethylsulfide photochemistry on methyl sulfur cycling in the equatorial Pacific Ocean. *Journal of Geophysical Research* 101 (2), 3715–3722.
- Kieber, D.J., Yocis, B.H., Mopper, K., 1997. Free-floating drifter for photochemical studies in the water column. *Limnology and Oceanography* 42 (8), 1829–1833.
- Kiene, R.P., Bates, T.S., 1990. Biological removal of dimethylsulfide from sea water. *Nature* 345, 702–705.
- Kiene, R.P., Hines, M.E., 1995. Microbial formation of dimethylsulfide in anoxic Sphagnum peat. *Applied and Environmental Microbiology* 61, 2720–2726.
- Kiene, R.P., Linn, L.J., 2000. The fate of dissolved dimethylsulfoniopropionate (DMSP) in seawater: tracer studies using ³⁵S-DMSP. *Geochimica et Cosmochimica Acta* 64, 2797–2810.
- Kiene, R.P., Service, S.K., 1991. Decomposition of dissolved DMSO and DMS in estuarine waters: dependence on temperature and substrate concentration. *Marine Ecological Progress Series* 76, 1–11.
- Lubin, D., Jensen, E.H., Gies, H.P., 1998. Global surface ultraviolet radiation climatology from TOMS and ERBE data. *Journal of Geophysical Research* 103, 26,061–26,091.
- Malmstrom, R.R., Kiene, R.P., Cottrell, M.T., Kirchman, D.L., 2004. Contribution of SAR11 bacteria to dissolved dimethylsulfoniopropionate and amino acid uptake in the North Atlantic Ocean. *Applied and Environmental Microbiology* 70 (7), 4129–4135.
- Mobley, C.D., 1994. *Light and Water: Radiative Transfer in Natural Waters*. Academic Press, San Diego.
- Morel, A., Maritorena, S., 2001. Bio-optical properties of oceanic waters: a reappraisal. *Journal of Geophysical Research* 106, 7163–7180.
- Neale, P.J., Davis, R.F., Cullen, J.J., 1998. Interactive effects of ozone depletion and vertical mixing on photosynthesis of Antarctic phytoplankton. *Nature* 392, 585–589.
- Nelson, N.B., Siegel, D.A., 2002. Chromophoric DOM in the open ocean. In: Hansell, D.A., Carlson, C.A. (Eds.), *Biogeochemistry of Marine Dissolved Organic Matter*. Academic Press, San Diego, pp. 547–578.
- Nelson, N.B., Siegel, D.A., Michaels, A.F., 1998. Seasonal dynamics of colored dissolved material in the Sargasso Sea. *Deep-Sea Research I* 45 (6), 931–957.
- Nightingale, P.D., Malin, G., Law, C.S., Watson, A.J., Liss, P.S., Liddicoat, M.I., Boutin, J., Upstill-Goddard, R.C., 2000. In situ evaluation of air-sea gas exchange parameterizations using novel conservative and volatile tracers. *Global Biogeochemical Cycles* 14, 373–387.
- Parsons, T.R., Maita, Y., Lalli, C.M., 1984. *A Manual of Chemical and Biological Methods for Seawater Analysis*. Pergamon Press, Oxford (173pp).
- Sakka, A., Gosselin, M., Levasseur, M., Michaud, S., Monfort, P., Demers, S., 1997. Effects of reduced ultraviolet radiation on aqueous concentrations of dimethylsulfoniopropionate and dimethylsulfide during a microcosm study in the lower St. Lawrence estuary. *Marine Ecological Progress Series* 149, 227–238.

- Saltzman, E.S., King, D.B., Holmen, K., Leck, C., 1993. Experimental determination of the diffusion coefficient of dimethylsulfide in water. *Journal of Geophysical Research* 98, 16,481–16,486.
- Shaw, G.E., 1983. Bio-controlled thermostasis involving the sulfur cycle. *Climate Change* 5, 297–303.
- Siegel, D.A., O'Brien, M.C., Sorensen, J.C., Konnoff, D.A., Fields, E., 1995. BBOP Data Processing and Sampling Procedures, Version 1. US JGOFS Planning Office, Woods Hole, MA.
- Simó, R., 2004. From cells to globe: approaching the dynamics of DMS(P) in the ocean at multiple scales. *Canadian Journal of Fisheries and Aquatic Sciences* 61 (5), 673–684.
- Simó, R., Dachs, J., 2002. Global ocean emission of dimethylsulfide predicted from biogeophysical data. *Global Biogeochemical Cycles* 16, 1078, doi:10.1029/2001GB001829.
- Simó, R., Pedrós-Alió, C., 1999a. Role of vertical mixing in controlling the oceanic production of dimethyl sulphide. *Nature* 402, 396–399.
- Simó, R., Pedrós-Alió, C., 1999b. Short-term variability in the open ocean cycle of dimethylsulfide. *Global Biogeochemical Cycles* 13, 1173–1181.
- Slezak, D., Herndl, G.J., 2003. Effects of ultraviolet and visible radiation on the cellular concentrations of dimethylsulfoniopropionate (DMSP) in *Emiliania huxleyi* (strain L). *Marine Ecology Progress Series* 246, 61–71.
- Slezak, D., Brugger, A., Herndl, G.J., 2001. Impact of solar radiation on the biological removal of dimethylsulfoniopropionate and dimethylsulfide in marine surface waters. *Aquatic Microbial Ecology* 25, 87–97.
- Smith, D.C., Azam, F., 1992. A simple, economical method for measuring bacterial protein synthesis rates in sea water using ³H-leucine. *Marine Microbial Food Webs* 6, 107–114.
- Steinberg, D.K., Carlson, C.A., Bates, N.R., Johnson, R.J., Michaels, A.F., Knap, A.H., 2001. Overview of the US JGOFS Bermuda Atlantic Time-series Study (BATS): a decade-scale look at ocean biology and biogeochemistry. *Deep-Sea Research II* 48, 1405–1447.
- Sunda, W., Kieber, D.J., Kiene, R.P., Huntsman, S., 2002. An antioxidant function for DMSP and DMS in marine algae. *Nature* 418, 317–320.
- Toole, D.A., Siegel, D.A., 2004. Light-driven cycling of dimethylsulfide (DMS) in the Sargasso Sea: closing the loop. *Geophysical Research Letters* 31, L09308, doi:10.1029/2004GL019581.
- Toole, D.A., Kieber, D.J., Kiene, R.P., Siegel, D.A., Nelson, N.B., 2003. Photolysis and the dimethylsulfide (DMS) summer paradox in the Sargasso Sea. *Limnology and Oceanography* 48, 1088–1110.
- Toole, D.A., Kieber, D.J., Kiene, R.P., 2004. White, E.M., Bisgrove, J., del Valle, D.A., Slezak, D., High dimethylsulfide photolysis rates in nitrate-rich Antarctic waters. *Geophysical Research Letters* 31, L11307, doi:10.1029/2004GL019863.
- van Rijssel, M., Gieskes, W.W.C., 2002. Temperature, light, and the dimethylsulfoniopropionate (DMSP) content of *Emiliania huxleyi* (Prymnesiophyceae). *Journal of Sea Research* 48, 17–27.
- Waters, K.J., Smith, R.C., Lewis, M.R., 1990. Avoiding ship-induced light-field perturbation in the determination of oceanic optical properties. *Oceanography* 3, 18–21.
- Wright, S.W., Jeffrey, S.W., Mantoura, R.F.C., Llewellyn, C.A., Bjornland, T., Repeta, D., Welschmeyer, N., 1991. Improved HPLC method for the analysis of chlorophylls and carotenoids from marine phytoplankton. *Marine Ecological Progress Series* 77, 183–196.
- Zemmelink, H.J., Dacey, J.W.H., Hints, E.J., 2004. Direct measurements of biogenic dimethylsulphide fluxes from the oceans: a synthesis. *Canadian Journal of Fisheries and Aquatic Sciences* 61 (5), 836–844.
- Zubkov, M.V., Fuchs, B.M., Archer, S.D., Kiene, R.P., Amann, R., Burkill, P.H., 2002. Rapid turnover of dissolved DMS and DMSP by defined bacterioplankton communities in the stratified euphotic zone of the North Sea. *Deep-Sea Research II* 49, 3017–3038.